PACS 61.82-BG; 61.66-DK; 62.20-FE

ALLOYS FOR MOLTEN-SALT REACTORS

V.M. Azhazha, A.S. Bakai, S.D. Lavrinenko, Yu.P. Bobrov, P.N. V'yugov, K.V. Kovtun, M.M. Pylypenko, V.I. Savchenko, A.D. Solopikhin, S.P. Stetsenko, D.G. Malykhin
National Science Center "Kharkov Institute of Physics and Technology",
1 Akademicheskaya St., 61108 Kharkov, Ukraine; E-mail: azhazha@kipt.kharkov.ua

Results are reported from studies on the selection, development and manufacture of structural materials for a fuel-salt circulation loop of molten-salt reactors. Studies into the properties of materials obtained were performed. The analysis of the main physical properties has suggested the nickel-based alloy with the optimum composition. The basic initial components of the alloy were refined by physical methods. The influence of deformation and thermal treatment on structural and mechanical properties of melted alloys was investigated. The present results give grounds to advise the alloys under discussion as materials for the fuel loop of molten-salt reactors.

1. INTRODUCTION

The nuclear power is a strategically important component of energy supply in Ukraine: its current and predicted contributions make about 50 % of the total electric power production. Along with the work aimed at extending the service life of operating reactors, the concept of nuclear-power engineering development anticipates the studies on advanced nuclear technologies and creation of new-type reactors which will form the basis for the development of nuclear power engineering in the coming years. Here, a high-temperature molten-salt reactor (MSR) seems to be the most promising and safe type of nuclear reactors. Aside from electric energy production, this reactor is capable of realizing afterburning of spent fuel. The MSR may operate at temperatures up to 1000°C and a fuel mixture pressure of a few atmospheres in the circulation loop. The salt melt of lithium/sodium/zirconium fluorides with additives of uranium or plutonium fluorides serves to be a fuel in the MSR.

The development of the MSR much depends on the progress in creating such structural materials that should meet a number of special requirements:

- a high corrosion resistance of fluoride salt melts;
- sufficient radiation resistance;
- adequate high-temperature strength;
- good manufacturability (ability to be deformed, machined, welded, etc.).

The aim of the present work was to choose, develop and manufacture the structural materials for the fuel-salt circulation loop of molten-salt reactors, and to investigate the properties of the materials obtained.

2. CHOICE OF THE MATERIAL AND METHODS OF ITS PRODUCTION

Nickel, molybdenum, chromium, iron and alloys on their base were considered as main materials-candidates for structural materials of the circulation loop. From the consideration and analysis of the main physical-chemical properties of the mentioned materials we have given preference to nickel-base alloys with molybdenum and chromium [1-4].

Nickel is used in many technically important alloys. Alloys with a diversity of properties (structural, heat-, corrosion-, and radiation-resistant alloys) are made on its base. Typical of nickel is the combination of high corrosion resistance in many aggressive media with high mechanical properties, as well as good workability in hot and cold states. Owing to this, nickel provides a basis for corrosion-resistant and heat-resistant alloys. Such elements as molybdenum and chromium may be dissolved in great amounts in nickel. Nickel exists in two modifications: β-Ni with the fcc lattice and α-Ni with the hcp lattice, which can be obtained by electrolysis only (at vacuum distillation). Its properties are essentially dependent on the content of impurities such as sulfur, carbon, phosphorus, oxygen, etc. The main physical and mechanical properties of nickel are presented in Table 1.

Molybdenum is characterized by high values of melting temperature, strength at high temperatures, corrosion resistance. Therefore, molybdenum is one of the most important alloying elements; it also makes the basis for many corrosion-resistant and high-temperature alloys. The main physical properties of molybdenum are given in Table 1.

Table 1

Main physical and mechanical properties of nickel, chromium, molybdenum and iron [2]

Metal	T_m, °C	$\alpha\cdot10^6$, K^{-1} 0…100°C	λ, W/(m·K)	$\rho\cdot10^6$, Ohm·cm	d, g/cm^3	H_B, MPa	$\sigma_в$, MPa	δ,%
Ni	1453	13.5	0.61	7.2	8.9	730	450*	50
Cr	1878	6.2	0.66	12.9	7.2	1000	281*[2]	0
Mo	2625	5.0	1.42	5.7	10.0	2200	370*[3]	–
Fe	1539	11.7	0.71	10.0	7.86	700	200	40

ВОПРОСЫ АТОМНОЙ НАУКИ И ТЕХНИКИ. 2005. №.4.
Серия: Физика радиационных повреждений и радиационное материаловедение (87), с. 40-47.

* – annealed nickel NP4, *[2] – recrystallized chromium iodide, *[3] – cast molybdenum of vacuum arc remelting.

Molybdenum has a high corrosion resistance in non-oxidative media and alkaline melts in wide ranges of temperatures and concentrations. It does not practically interact either with cold and hot hydrofluoric and acetic acids of any concentrations or with solutions of hydrochloric and sulfuric acids at room temperature. Molybdenum is not resistant in oxidative media. The presence of even small additions of oxidizers in the acid leads to a drastic deterioration of its corrosion resistance. Molybdenum is stable in the melts of sodium up to 1500°C, bismuth up to 1472°C, lead up to 1100° C, lithium and potassium up to 900°C.

Chromium has a high melting temperature, shows the ability to passivation and a high resistance to oxidation. These properties are transferred to steels and alloys, where chromium enters into the composition. Therefore, chromium is the main alloying element of corrosion-resistant high-temperature heat-resistant alloys. Of all three possible modifications of chromium (α, β, and γ), the α-modification having the bcc lattice is the most stable. The main physical and mechanical properties of chromium are given in Table 1. Chromium has a strong affinity with oxygen, nitrogen and carbon. The solubility of nitrogen in it at 1200°C makes $8.7 \cdot 10^{-2}$ %. Owing to the passivation phenomenon, chromium is stable in oxidative media. For example, the concentrated nitric, phosphoric, chloric acids form oxide films on chromium, and this leads to its passivation. Chromium reacts with anhydrous halogens: hydrogen chloride and hydrogen fluoride. Water solutions of hydrofluoric acid and hydrochloric acid, hydrogen bromide and hydrogen iodide dissolve chromium in the same way as weak sulfuric acid does.

Nickel-base alloys. The present-day corrosion-resistant nickel alloys, which can be well deformed and welded, belong to three main alloying systems: Ni-Mo, Ni-Cr, Ni-Cr-Mo [2]. The nickel-base alloys show a higher corrosion resistance to fluoride melts than the iron-base alloys. Simultaneous alloying of nickel with chromium and molybdenum makes it possible to create ultrahigh-resistance alloys in a wide range of corrosive active media of oxidation/reduction character. Along with a high corrosion resistance, the alloys show an exceptional resistance to local types of corrosion (intercrystalline, crevice, pitting, corrosion cracking, etc.). Besides, these alloys are heat-resistant at high temperatures. They combine high strength and plasticity from temperatures below zero to 1200°C.

The effect of mutual effect of chromium and molybdenum on the corrosion resistance of the alloy is determined by the properties of aggressive medium. In oxidative media, the corrosion resistance of alloys increases mainly do to an increase in chromium concentration there, and in reducing media – due to increase in molybdenum content.

The maximum resistance to total corrosion is shown by the alloys in the homogeneous state (γ-solution quenching). Depending on the aggressive medium (composition, temperature, oxidation-reduction potential), the heterogeneous structure determined by the presence of carbide phases leads to the reduction in corrosion resistance of alloys. The chemical composition of some nickel-base alloys is given in Table 2.

Table 2

Chemical composition of typical nickel-base alloys

Alloy brand	Chemical composition, wt. %						Other elements
	Ni	Mo	Cr	Fe	Ti	Al	
Kh20N80 (nichrome)	77	–	20	rest	–	≤0.2	C≤0.15
KhN77TYu	Base stock.	–	21	–	2.5	0.75	Ce≤0.01 C≤0.06
KhN75VMFYu	75	~5.7	10	≤5.0	–	4.3	W~5; B – 0.01…0.02; V~0.7
KhN80TBYu	Base stock.	–	16	≤3.0	2.1	0.8	Nb~1.25; C<0.08
KhN80MTYu	Base stock.	–	5.5	–	0.01	1.03	Mn-0.03 Nb-12.3
Hastelloy C	Base stock.	1.6	22	6	–	–	W~4.5; C<0.12
Hastelloy X	45	9	22	20	–	–	C<0.15
Hastelloy N	71	16	7	≤5.0	Al+ Ti ≤ 0.35		Co≤0.20; Cu≤0.35 W≤0.50; C<0.08 Mn<0.8
Hastelloy N modified	Base stock.	11…13	6…8	≤0.1	≤2.0	≤0.1	Co≤0.20; Cu≤0.10 C<0.10; Nb-0...2 Mn-0.1…0.25

The growth of intercrystalline corrosion of Ni-Cr-Mo alloys is determined by precipitation of molybdenum- and chromium-enriched carbide and intermediate phases along the grain boundaries in the form of interconnected precipitates. In other words, to reduce intercrystalline corrosion in these alloys, it is necessary to increase the stability of their γ-solution at

the expense of a low content of carbon and silicon and a balanced content of chromium and molybdenum [2].

The improvement in the strength and heat resistance of alloys is provided by the formation of highly dispersed strengthening phases: intermetallic compounds, carbides and borides.

For operation in a molten-salt reactor, the alloy must have the following parameters: corrosion resistance in the $NaF+ZrF_4+UF_4$ salt melt at temperatures between 650 and 750°C, adequate radiation resistance and high mechanical characteristics at the mentioned temperatures. As it follows from the analysis of literature data, nickel alloys of Hastelloy N (modified) type and its Russian analog KhN80MT most fully meet these requirements. Proceeding from this, we have chosen high-nickel alloys of Hastelloy N type (for their composition, see Table 3) for melting, manufacture of structural materials and their subsequent studies. The difference in the chemical composition of alloys A and B lies in the fact that 0.5 wt. % of chromium in alloy B was replaced by niobium, and 0.05 wt. % of yttrium was introduced in addition.

Table 3

Chemical composition of alloys of Hastelloy-N Type

Alloy brand	Impurity content, wt. %						
	Ni	Mo	Cr	Fe	Ti	Al	Other elements
A	base stock.	11…12	6.5…7.5	≤1.5	≤ 0.5	≤ 0.8	Mn<0.5; Si<0.15
B	base stock.	11…12	6.2…7.2	≤1.5	≤ 0.5	≤ 0.8	Mn<0.5; Si<0.15; Nb – 0.5; Y – 0.05

The main difference of our alloys from the alloys-analogs was that for production of our alloys we have used high-purity initial components with a low content of interstitial impurities. The alloy components (nickel, molybdenum, chromium, iron, aluminum, titanium, manganese) were pre-freed of foreign substances by physical methods. Since these metals strongly differ in their properties, to remove impurities from them by one and the same method is impossible. Thus, to refine nickel, molybdenum, niobium, titanium and iron, the method of vacuum electron-beam melting (EBM) was used [5]. For refinement of chromium and aluminum we have used high-vacuum annealing. Manganese was refined by the vacuum distillation method. The refinement of metals as alloy components has resulted in the following.

Nickel. Electrolytic nickel, twice subjected to the EBM, was used as an initial material. As a result of refinement, the content of iron, cobalt, phosphorus, aluminum, magnesium has decreased; the decrease in the content of arsenic, zinc, selenium and chlorine was most substantial. The double EBM provided nickel of 99.994 wt. % purity [6].

Molybdenum. After the EBM, the content of metallic impurities has decreased by factors of 10 to 30. The removal of silicon was very insignificant. The tungsten impurity is not removed from molybdenum. Gaseous impurities (oxygen, nitrogen and hydrogen) were the main substances removed.

Niobium. Niobium NB-1 served as an initial material for melting. Upon two successive EBM it comprised the following impurities: Al – 0.004, Fe – 0.0001, Cr < 0.001, Ni < 0.0004, Si – 0.005, Cu – 0.0006, Ca < 0.003 wt. %.

Titanium. Titanium sponge TG-90 was used as an initial material for melting. The EBM method gave a titanium ingot of 99.99 wt. % purity.

Iron. Armco-iron rods were used as an initial material for melting. The EBM of iron was performed by drop remelting. The Brinell hardness of the rods before melting was 830 MPa, after the refinement it decreased down to 624 MPa. The iron purity level was essentially determined by the content of nickel and cobalt.

Chromium. Iron, silicon, aluminum, nickel, and also interstitial impurities such as nitrogen, oxygen and carbon are the main foreign substances in chromium. A high-vacuum annealing of chromium samples at 1200°C for 5 hours has decreased the content of interstitial impurities by a factor of about 10.

The high-purity metals obtained were used to prepare previously weighed samples for melting alloys in accordance with the percentage of the Hastelloy-type alloy. The corresponding data are presented in Table 4.

Table 4

Percentage of alloy components

Element	Alloy A		Alloy B	
	weight, g	content, wt.%	weight, g	content, wt.%
Nickel	1053.9	78.15	1082.7	78.15
Molybdenum	157.78	11.7	162.1	11.7
Chromium	110.58	8.21 (6.7)*	106.68	7.71 (6.2)
Titanium	7.69	0.57 (0.47)	7.8	0.57 (0.47)
Aluminum	16.0	1.22 (0.83)	16.44	1.22 (0.83)
Iron	20.23	1.5	20.78	1.5
Manganese	8.95	0.63 (0.5)	9.19	0.63 (0.5)

Silicon	2.7	0.2 (0.15)	2.77	0.2 (0.15)
Niobium	–	–	6.93	0.5
Yttrium	–	–	0.7	0.05

** The values in parentheses correspond to the calculated concentrations with due account for the burnup of the components during alloy smelting.*

The induction melting and casting were performed in the argon environment of the vacuum induction furnace "Kristall-603" using the fine gas cleaning facility that has sorption and getter filters. The 0.5 *l* alundum crucible was loaded with initial alloy components subjected to refinement, namely, nickel, molybdenum, chromium, titanium, iron and niobium. After the crucible was heated to a temperature of 1000°C in vacuum $6 \cdot 10^{-3}$mm Hg, a purified argon was let in to a pressure of 400 mm Hg. Then the temperature was elevated up to 1600°C. At these conditions, the alloy components were melted and mixed in a liquid state. On holding the alloy for 10 minutes, the previously prepared and weighed samples of manganese with aluminum and silicon (alloy A) or manganese with aluminum and yttrium followed by silicon (alloy B) were added into it. Within 2 minutes after the introduction of the last component, the alloy was poured through the drain hole in the bottom part of the crucible into a copper water-cooled mold, thereby minimizing the size of the shrinkage void and decreasing the segregation effect in the multicomponent alloy. In this way alloy ingots, 80 mm in diameter and 20 mm in height, were produced [7].

By spark cutting of ingots, prismatic billets were obtained for rolling that was carried out in air at elevated temperatures. The billet was preheated to a temperature of 900°C, and then was rolled in air to a thickness of 1 and 0.3 mm with intermediate heatings. The rolled stock was electrically cut to prepare samples of required shape for conducting further investigations.

The samples to be investigated underwent the following thermal treatment: 1 – heating to a temperature of 1100°C, 1 hour exposure interval and water quenching; 2 – aging at 675°C for 50 hours in argon atmosphere.

The composition of initial components and alloys obtained after induction melting was determined by the methods of laser mass-spectrometry (EhMAL-2 device) and chemical analysis. The microstructure of samples was examined with the optical microscope MMR-4, the microhardness was measured with the PMT-3 device. The alloys were mechanically tested at the tensile machine of type 1246R-2/2600 in the temperature range from 20 to 650°C. The temperature dependence *E(T)* was measured using the IVT-3 device. X-ray diffraction studies of alloys were performed at DRON4-07 device with the scintillation counter in CuKα and CoKα radiation. Photographs were taken using the Bragg-Brentano optical schematic.

3. RESULTS AND DISCUSSION

The microstructure of alloy samples and its transformation were investigated as functions of the state of the sample, i.e., after casting, deformation and the corresponding type of heat treatment. Figure 1 shows the alloy microstructure after casting and subsequent homogenizing annealing for 6 hours at 1000°C in vacuum. It can be seen that the homogenizing annealing leads to an increase in the grain size.

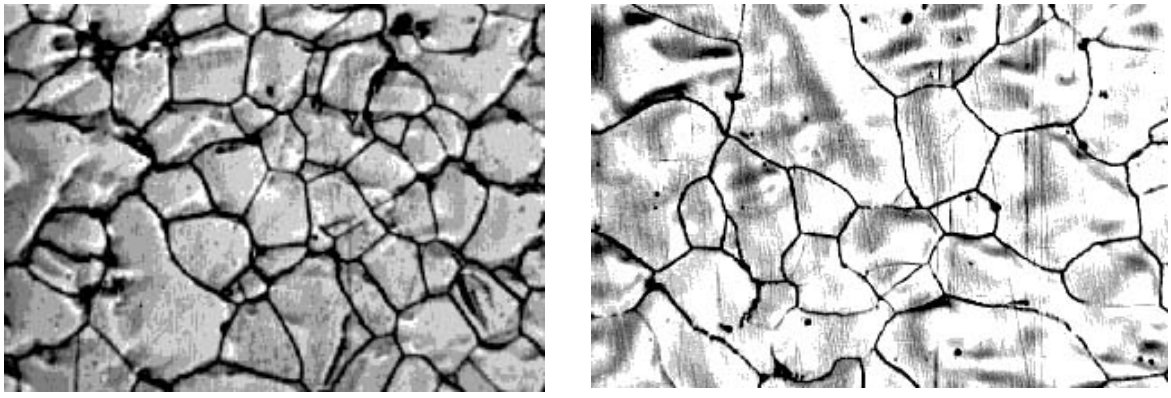

a *b*

Fig. 1. Microstructure of Hastelloy-type alloy: a – after casting; b – after homogenizing annealing (200x magnification)

The microstructure of Hastelloy-type alloy samples in different planes relative to the direction of rolling is shown in Fig. 2 in the as-rolled state and after various heat treatments. It can be noted that in the as-rolled state a clearly marked grain structure is seen only on the wide part of the sample in the rolling plane. The quenching gives rise to the structure typical of high-nickel alloys.

Figure 3 shows the structure of the Hastelloy-type alloy samples after water quenching from a temperature of 1100°C (Fig. 3,a) and after the subsequent aging at 675°C for 50 hours in the argon atmosphere (Fig. 3,b). The comparison between the alloy structures shows that depending of heat treatment conditions, the excess carbide and intermetallic phases may be distributed in the alloy structure as separate or relatively interconnected particles at grain boundaries or in the grain bulk. The 50-hour aging of alloys at 675°C leads to an increase in the volumetric part of precipitates and to the formation

of interconnected precipitates, and also, to an increase in the grain size.

The microhardness measurements of alloy samples in different planes relative to the rolling direction and after different types of heat treatment have shown no appreciable anisotropy in the microhardness of the alloys under study. The type of samples heat treatment, in particular, making the alloy aging, substantially affects the microhardness value. Thus, the microhardness of as-rolled samples is 2620 MPa, while after quenching this value decreases down to 2395 MPa, and after quenching and aging it increases up to 2860 MPa. The increase in alloy hardness at aging is peculiar to many metastable metallic materials which experience the decay of the supersaturated solid solution, and is due to structural transformations at stages of excess phase formation [8].

The undertaken X-ray diffraction studies of alloys have permitted us to determine the lattice spacings, the dimensions of coherent scattering areas (CSA) and the level of microdistortions (ε) in alloy samples after various treatments. The measured data are listed in Table 5. It is obvious from the table that the lattice spacing is the parameter sensitive to the type of treatment. The subsequent aging initiates the inverse process.

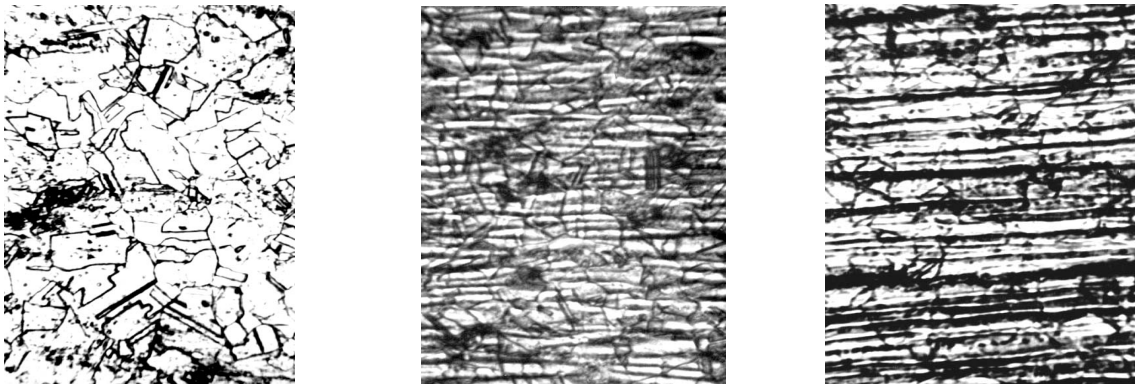

a

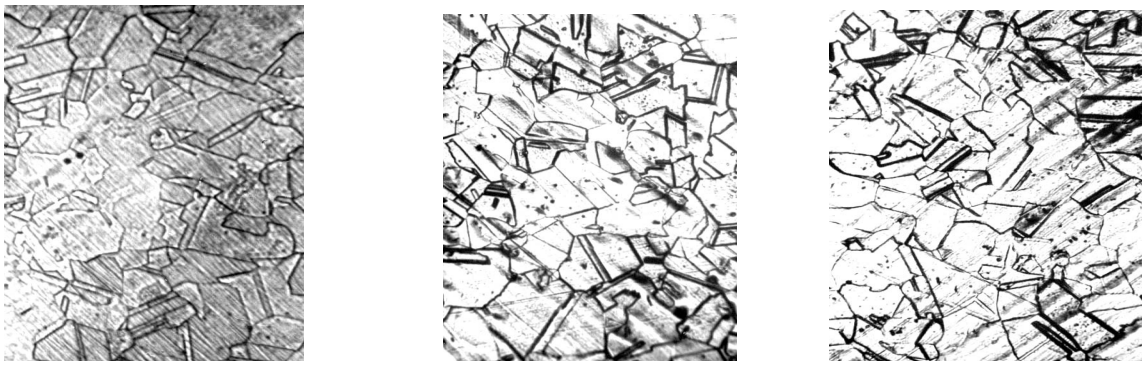

b

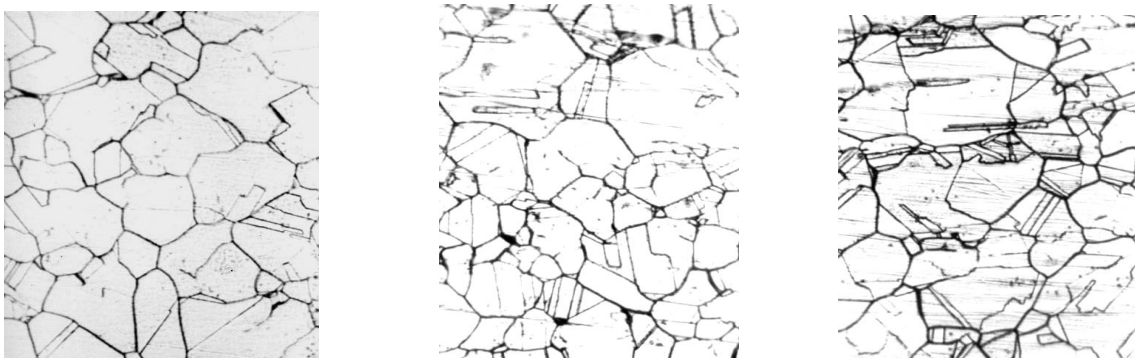

c

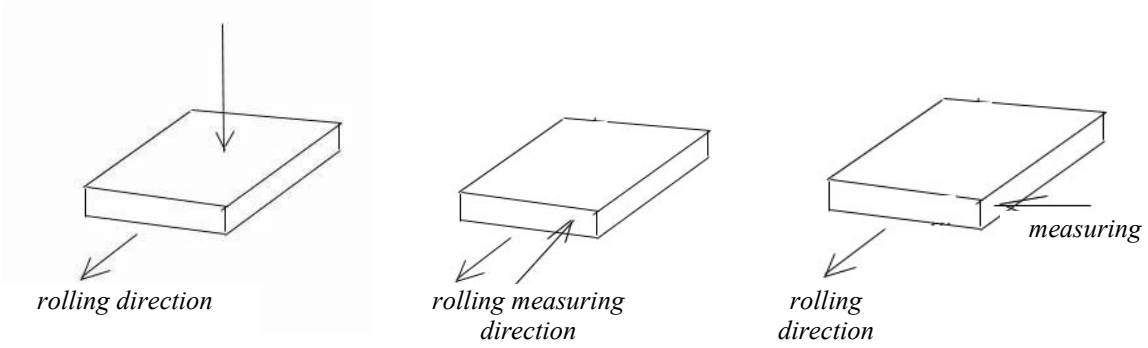

Fig. 2. Microstructure of Hastelloy-type alloy samples in different planes relative to the rolling direction: a - rolled ingot, b – rolled and quenched ingots, c – rolled, quenched and aged ingots (380x magnification)

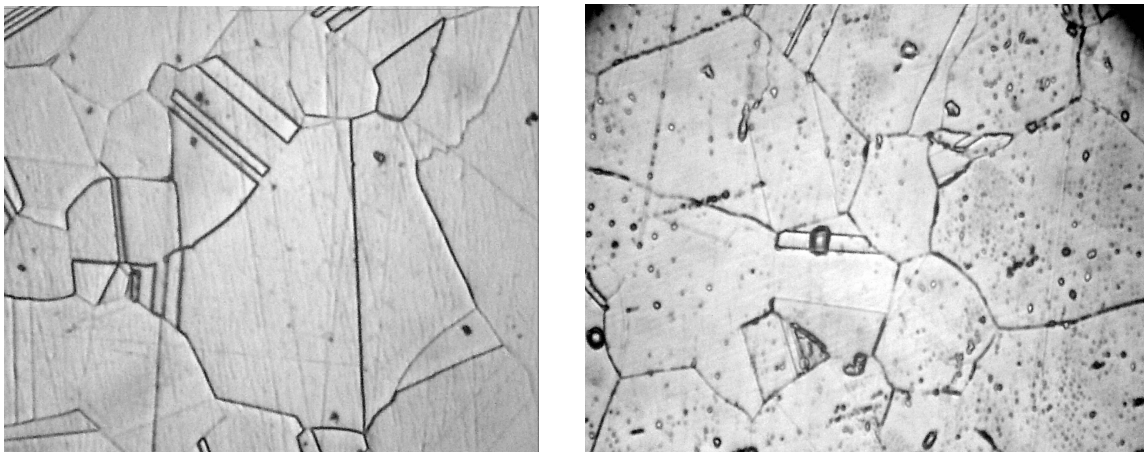

a *b*

Fig. 3. Microstructure of alloy A samples: a – after annealing in air for 1 hour at 1100°C and water quenching; after water quenching and annealing for 50 hours at 675°C (aging) in the argon atmosphere (1100x magnification)

Table 5

Lattice spacings (*a*), CSA dimensions (*D*) and the level of microdistortions (ε) in alloys A and B in the initial state, after quenching and aging of quenched alloys

Treatment type	Alloy A			Alloy B		
	a (nm)	*D* (nm)	$<\varepsilon^2>^{1/2} \cdot 10^3$	*a* (nm)	*D* (nm)	$<\varepsilon^2>^{1/2} \cdot 10^3$
Initial	0.3580	17	2.9	0.3580	29	3.65
Quenching	0.3562	18.5…24	2.8…3.05	0.3567	17.5…19	2.25…2.35
Quenching + aging	0.3568	17…24	1.65…2.1	0.3573	20.5…22.5	2.35…2.45

From the behavior of substructure parameters it can be concluded that at the microstructural level alloy A is more plastic than alloy B. It can be seen from the level of microdistortions in the initial (strained) state and the aged state. A substantial decrease in the ε value is an indicator of completion of the aging process. From this point of view, the process of aging (in its classical meaning) in alloy B is probably not completed.

The mechanical properties of alloy samples are presented in Table 6. It is seen that the samples subjected to different kinds of heat treatment after rolling differ in their mechanical properties. It should be noted that the σ_B value for alloy B is somewhat less than for alloy A after two kinds of heat treatment. This is evidently due to some distinctions of structural transformations in the alloys at their heat treatment, caused by variations in the chemical composition of the alloys.

Table 7 and Fig. 4 give the data on variations in the mechanical properties of alloys versus aging time.

Table 6

Mechanical properties of Hastelloy-type alloys at room temperature

Property	Heat treatment conditions					
	after rolling		after rolling and water quenching		after rolling, water quenching and aging	
	Alloy A	Alloy B	Alloy A	Alloy B	Alloy A	Alloy B
σ_B, MPa	1450	1470	930	880	870	810
$\sigma_{0,2}$, MPa	1350	1400	358	345	433	465
δ, %	3…5	3...5	60	63	65	43

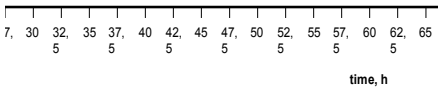

a *b* *c*

Fig. 4. Mechanical properties of Hastelloy-type alloys versus aging time: a - σ_B, MPa; b – $\sigma_{0,2}$, MPa; c – δ, %

Table 7

Mechanical properties of Hastelloy-type alloys versus aging time

	Aging time, h	σ_B, MPa	$\sigma_{0,2}$, MPa	δ, %
Alloy A	0	930	358	60
	50	870	433	65
	70	913	527	55
	100	854	479	40
Alloy B	0	880	345	63
	50	810	465	43
	70	845	443	40
	100	840	494	32

The yield strength value of the alloys after aging is appreciably greater than that of the alloys subjected to quenching only. The yield strength before aging corresponds to the yield strength of a supersaturated solid solution. The bulk part of precipitates grows with aging, and since the particle size is very small, the increase in the yield strength is approximately proportional to the cubic root of the volumetric content of the precipitated phase [9, 10]. As aging goes on, the particles produced begin to grow and at some moment they loose coherency with the matrix. Simultaneously, the effective volumetric part of precipitates decreases. As this process occurs gradually, no decrease in the yield strength takes place, though its development with aging time slows down. Relying on the data in Table 5 it can be stated that the cause of plasticity reduction in the alloys under study is connected with the formation of a great number of precipitates of intermetallic and carbide phases as a result of decay of supersaturated solid solution at aging. The precipitates formed present obstacles to the motion of dislocations, thereby affecting the plasticity of the material. As compared to alloy A, the plasticity value of alloy B is lower, this being evidently due to a great number of precipitates formed at aging at the expense of a greater number of alloying components in this alloy (see Tables 1 and 2). The pattern of structural changes that take place in alloys during their aging is rather many-sided, and from the results of previous studies no unambiguous conclusions can be drawn about the cause of plasticity reduction in the alloys under study.

In the measurements of the coefficient of elasticity as a function of temperature, *E(T),* we have used flat thin samples, where transverse resonance oscillations were excited. The coefficient of elasticity was calculated in this case by the following formula

$$E = 0{,}965 \cdot 10^{-3} \left(\frac{L}{h} \right)^3 \frac{P f_r^2}{b}, \quad (1)$$

where L is the length of the sample (cm); h, b are, respectively, the width and thickness of the sample (cm); P is the sample's weight (kg); f_r is the resonance frequency of bending vibrations (Hz).

The temperature dependence $E(T)$ was determined in the temperature range from 80 to 300 K at heating the sample precooled to a liquid nitrogen temperature. The measurements were performed on one sample of the alloy that was subjected to various heat treatments. The test results are shown in Fig. 4. According to the measuring technique, the ductile-to-brittle transition temperature was determined as a middle of resonance frequency jump, i.e.:

$$T_x = 0{,}5\ (T(f_{r\,min}) - T(f_{r\,max})), \quad (2)$$

where $T(f_{r\ max,\ min})$ is the is the temperature value corresponding to the maximum and minimum resonance frequency.

From the curves shown in Fig. 5 it is rather difficult to discriminate the T_{br} parameter. The cold brittleness temperature can be determined more exactly and clearly, if the resonance frequency variations are normalized as follows:

$$f_{reduced} = (f_{max} - f_{current})/(f_{max} - f_{min}),\ \%. \quad (3)$$

The reconstructed curves are presented in Fig. 6.

As it follows from Figs. 5 and 6, the cold brittleness temperature for samples 1, 2, 3, 4 makes 200, 246, 241 and 216 K, respectively. The measurement accuracy is found to be ±5 K. It is obvious that the quenching of the alloy sample decreases the cold brittleness temperature value. A subsequent aging displaces the cold brittleness temperature to the lower temperature region. The initial sample has a higher coefficient of elasticity, this being due to a stressed state of the alloy after rolling. In the process of heat treatment, stress relaxation and grain structure changes take place, that leads to a decrease in the coefficient of elasticity. At a later time the modulus E of quenched and aged samples remains practically unchanged (see Fig. 5, curves 2, 3, 4).

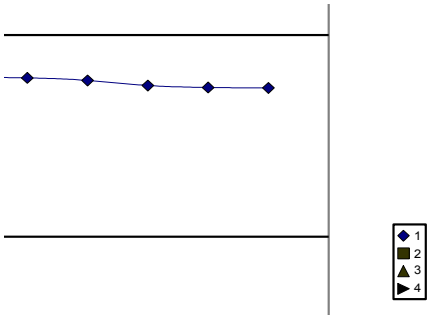

Fig. 5. Resonance frequency variation at heating of Hastelloy-type alloy samples subjected to different heat treatments: 1 – initial sample, 2 – sample after quenching, 3 – after aging at 675°C for 70 hours, 4 – after aging at 675°C for 100 hours

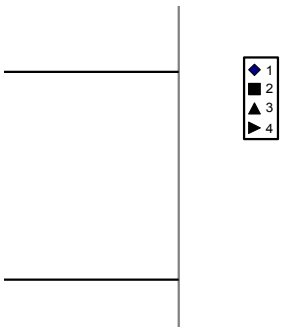

Fig. 6. Reduced resonance-frequency variations at heating of Hastelloy-type alloy samples after various heat treatments. The numbers of curves are the same as in Fig. 5. $f_{reduced} = (f_{max} - f_{current})/(f_{max} - f_{min})$, % is plotted on the ordinate

The present investigations suggest the conclusion that the two alloys A and B have demonstrated high mechanical properties and can be proposed as a material-candidate for the fuel loop of molten-salt reactors. The subsequent comprehensive studies into mechanical, corrosion and radiation properties of these alloys will make it possible to choose with certainty the alloy of optimum composition [11].

4. CONCLUSIONS

1. High-purity metals were used to melt two alloys (A and B).
2. The analysis performed on the main physical and chemical properties of candidate materials for the MSR fuel loop confirm the commonly accepted opinion that the Hastelloy N-type alloys are suitable for the MSR.
3. The results of investigations of chemical composition, structure and mechanical properties of the alloys at different stages of deformation and heat treatment show that the two variants of alloys have good mechanical properties and can be used as a structural material for the fuel loop of molten-salt reactors.

This work was partially supported by the STCU, Project #294.

REFERENCES

1.V.M. Novikov, V.V. Ignat'ev, V.I. Fedulov, V.N. Cherednikov. *Molten-salt nuclear energy devices: prospects and problems* (in Russian). Moscow: "Ehnergoizdat publ.", 1990, 192 p.

2.E.A. Ul'yanin, T.V. Svistunova, F.L. Levin. *High corrosion-resistance alloys* (in Russian). Moscow: "Metallurgiya publ.", 1987, 88 p.

3.N.M. Beskorovainy, Yu.S. Benomptsev, M.D. Abramovich, et al. *Structural materials of nuclear reactors* (in Russian). Moscow: "Atomizdat publ.", 1977, 256 p.

4.V.L. Blinkin, V.M. Novikov. *Molten-salt nuclear reactors* (in Russian). Moscow: "Atomizdat publ.", 1978, 112 p.

5.G.F. Tikhinsky, G.P. Kovtun, V.M. Azhazha. *Production of superhigh-purity rare metals* (in Russian). Moscow: "Metallurgiya publ.", 1986, 160 p.

6.V.M. Azhazha, Yu.P. Bobrov, V.D. Virich, et al. Refinement of nickel by electron-beam melting (in Rus-

sian) // *Kharkov University Bulletin*. Ser. fiz. “Yadra, chastynky, polya”. 2003, # 601, iss. 2(22), p. 118–122.
7.V.M. Azhazha, Yu.P. Bobrov, A.F. Vanzha, P.M. V’yugov, T.G. Yemlyaninova, K.V. Kovtun, S.D. Lavrinenko, M.M. Pylypenko, V.I. Savchenko, A.D. Solopikhin, S.P. Stetsenko. Development of the alloy for the MSR fuel loop (in Ukrainian) //*Kharkov University Bulletin*. Ser. fiz. “Yadra, chastynky, polya”. 2004, N 619, iss.1(23), p. 87–93.
8.A.P. Gulyayev. *Physical metallurgy* (in Russian). Moscow: “Metallurgiya publ.”, 1978, 645 p.
9.V.I. Trefilov, V.F. Moiseev. *Disperse particles in refractory metals* (in Russian). Kiev: “Naukova Dumka publ.”, 1978, 240 p.
10.K.I. Portnoy, B.N. Babich. *Dispersion-strengthened materials* (in Russian). Moscow: “Metallurgiya publ.”, 1974, 200 p.
11.V. Azhazha, A. Bakai, S. Lavrinenko, Yu. Bobrov, et al. Alloys for molten-salt reactors (in Ukrainian) // *Proc. XVI Int. Conf. on Physics of Radiation phenomena and Radiation Material Science. 6-11 September, 2004, Alushta, Crimea.* NSC KIPT, p. 271–272.

СПЛАВЫ ДЛЯ ЖИДКО-СОЛЕВЫХ РЕАКТОРОВ

В.М. Ажажа, А.С. Бакай, С.Д. Лавриненко, Ю.П. Бобров, П.Н. Вьюгов, К.В. Ковтун, Н.Н. Пилипенко, В.И. Савченко, А.Д. Солопихин, С.П. Стеценко, Д.Г. Малыхин

Приведены результаты исследований по выбору, разработке и изготовлению конструкционных материалов для контура циркуляции топливной соли жидко-солевых реакторов и исследованию свойств, полученного материала. Анализ основных физических свойств позволил выбрать сплав на основе никеля с оптимальным составом. Проведено рафинирование физическими методами основных исходных компонентов сплава. Изучено влияние деформации и термической обработки на структурные и механические свойства полученных материалов. Полученные результаты позволяют рекомендовать эти сплавы в качестве материалов для топливного контура жидко-солевых реакторов.

СПЛАВИ ДЛЯ РІДИННО-СОЛЬОВИХ РЕАКТОРІВ

В.М. Ажажа, О.С.Бакай, С.Д. Лавриненко, Ю.П. Бобров, П.М. В’югов, К.В. Ковтун, М.М. Пилипенко, В.І. Савченко, А.Д. Солопіхін, С.П.Стеценко, Д.Г.Малихін

Приведено результати досліджень по вибору, розробці та виготовленню конструкційних матеріалів для контуру циркуляції паливної солі рідинно-сольових реакторів і дослідження властивостей, отриманого матеріалу. Аналіз основних фізичних властивостей надав перевагу сплавам на основі нікелю. Вибрано оптимальний склад сплаву. Проведено рафінування фізичними методами основних вихідних компонентів сплаву. Вивчено вплив деформації та термомеханічної обробки на структурні та механічні властивості отриманих матеріалів. Отримані результати дозволяють рекомендувати ці сплави в якості матеріалів для паливного контуру рідинно-сольових реакторів.